



# Multi-parameter logging evaluation of tight sandstone reservoir based on petrophysical experiment

Haitao Li<sup>1</sup> · Shaogui Deng<sup>1</sup> · Feng Xu<sup>4</sup> · Yunfeng Niu<sup>2</sup> · Xufei Hu<sup>3</sup>

Received: 10 August 2020 / Accepted: 21 January 2021 / Published online: 7 February 2021  
© Institute of Geophysics, Polish Academy of Sciences & Polish Academy of Sciences 2021

## Abstract

Acoustic, resistivity and nuclear magnetic resonance (NMR) logging are important means of reservoir evaluation. In this paper, the information of pore structure, such as the aspect ratio and the shape, is obtained by rock physical experiments like constant velocity mercury injection and casting thin section. Taking pore structure information as a link, the theoretical relations among acoustic-NMR, acoustic-resistivity and resistivity-NMR of rocks are studied, respectively, based on the differential equivalent model and fractal theory, and the theoretical derivation results are verified by AE acoustic emission experiment, rock resistivity experiment and NMR experiment. It is found that there is a power function relationship between the P/S wave velocity and the geometric mean value of NMR  $T_2$ . Moreover, there are also power function relationships between the slowness of P/S wave and resistivity, and between the value of NMR  $T_2$  and the increase rate of resistance. Based on the above relationship, the gas reservoir can be identified by acoustic-resistivity-NMR multi-parameters in well G of the study area. Compared with the conventional P/S velocity ratio and P-wave slowness intersection method, the separation effect of gas and water is more obvious.

**Keywords** Petrophysical experiment · Pore structure · Acoustic-resistivity-NMR parameters relationships · Gas identification

## Introduction

The exploration and development of complex oil and gas reservoirs need to use a variety of logging parameters to obtain more accurate stratigraphic information (Han et al. 2016; Yin et al. 2016; Zhu et al. 2015). It is one of the important means to evaluate the reservoir by the combination of acoustic, resistivity and NMR logging methods (Li

et al. 2018; Hamada et al. 2001). However, the pore structure of rock affects the response characteristics of acoustic, resistivity and NMR logging. Mercury injection, CT scanning, nuclear magnetic resonance and other experiments show that pore structure is a series of pores and throats with different sizes and shapes (Guo et al. 2019; Xu et al. 2018; Oluwadebi et al. 2019). Prasad (2001) showed that the shape of the pore changed the sound velocity and elastic modulus by influencing the propagation path of the wave. Kumar and Han (2005) thought that the increase in spherical pore content made the sound velocity of the model quite different from that of Wyllie time average (Wyllie et al. 1956). Combined with thin section and resistivity experiments, Verwer et al. (2011) found that under the same porosity condition, the larger the number of pores, the larger the cementation index and small pores and complex pore structure make the cementation index decrease in carbonate rocks. Based on the rock particle accumulation model, Wang et al. (2004) used Monte Carlo and random walking algorithm to obtain the NMR response under certain magnetic field conditions. Liu et al. (2012) used the spherical tube model to numerically simulate the conductivity of different pore structures, proving that

---

Communicated by Michal Malinowski (CO-EDITOR-IN-CHIEF)/Jadwiga Anna Jarzyna, prof (ASSOCIATE EDITOR).

✉ Shaogui Deng  
854938905@qq.com

<sup>1</sup> School of Geosciences, China University of Petroleum, Qingdao 266580, Shandong, China

<sup>2</sup> Institute of Electronics, Chinese Academy of Sciences, Beijing 100190, China

<sup>3</sup> Faculty of Petroleum, China University of Petroleum-Beijing At Karamay, Karamay 834000, China

<sup>4</sup> Development of Jidong Oilfield, Research Institute of Petroleum Exploration, Tangshan 063000, China

pore structure is one of the factors leading to the resistivity divergence though the experimental data. In this paper, the sandstone samples located in Gaobei slope of Huanghua Sag are selected, which basic information is shown in Table 1, to carry out the joint acoustic, resistivity and NMR experiment. The pore structure of samples is classified by fractal theory and principal component analysis method (Chen et al. 2013; Cao et al. 2016; Guo et al. 2018; Zhang et al. 2017), and then the theoretical relationship between acoustic, resistivity and NMR parameters is studied with the help of numerical simulation and the results of rock physical experiment, which assists the evaluation of tight sandstone gas reservoir by multi-logging parameters.

## Experimental measurement and data analysis

### Acoustic-Resistivity joint experiment, NMR and Mercury injection experiment measurement

All samples were placed in a 110°C drying machine for 24 h after washed with oil and salt, and then samples are fully saturated under 30 MPa pressure in MPC-II saturation instrument with NaCl solution salinity of 4,000 mg/L for 48 h which is determined by average actual formation water resistivity test. An HSN-B intelligent acoustic velocity-resistivity measuring device is used to measure the P-wave and S-wave velocities and resistivity of the saturated samples under normal conditions, which is due to the pressure of the layer where the sample located is about 25 MPa, there is no significant change in the acoustic velocity of the sample measured in the laboratory under this pressure. Saturated samples NMR signal is measured with a spin-echo pulse sequence by using a 2 MHz NMR Core Analyzer (Niumai IPC-801) from Niumai Electronic Technology Company. The measurements are carried out with inter-echo time spacing (TE) of 0.37 ms, waiting time (TW) of 6,000 ms, cumulative frequency of 128 Hz and echo number of 4,096. The test temperature is 25 °C. Moreover, the SIRT method is used for NMR T2 spectrum inversion with 5,000 iterations.

**Table 1** Samples basic parameters list

Core number	Well	Depth/m	Porosity/%	Permeability/ mD
1–13	X1	3471.5–4154.7	6.5–14.9/11.2	0.289– 2.881/1.411
14–22	X2	3217.6–3356.5	15.2–23.1/18.4	0.94– 9.785/3.558
23–34	X3	4214.1–5068.4	2.9–5.9/4.8	0.039– 1.189/0.412

After the above measurements are completed, a high-speed refrigerated centrifuge is used, and during centrifugation, the acoustic velocity and resistivity of the samples under different saturation are measured with the device until the water saturation of the sample does not change, indicating that the bound water state is reached, at this point, nuclear magnetic resonance T2 spectrum was measured again to obtain NMR signals in the state of bound water, after which the experiment is stopped.

Mercury injection experiment is to make mercury enter the pore through pressure, and the energy required for pore volume increment is equal to the work done by external force. The volume and specific surface area of the cylindrical hole are calculated according to the relationship between pressure and capacitance, and the pore size distribution is calculated according to Washburn equation. The poremeter-33 automatic measuring device was used in this experiment. During the experiment, the sample was first weighed and sealed in the sample tube. The low-pressure test was carried out in the low-pressure station, and then the sample tube was taken out in the high-pressure station for high-pressure measurement. After the measurement, the experimental data of samples were obtained and the samples were taken out.

### Data analysis

#### (1) Relationship between acoustic velocity and NMR T2gm

Based on measurement of P/S wave velocity and NMR standard T2 experiments under different porosity conditions, the cross-plot of the P/S wave velocity and the geometric mean value of T2 under different porosity conditions are obtained, as shown in Fig. 1. The experimental results show that there is a power function relationship between P/S wave velocity and T2gm.

#### (2) Relationship between resistivity and acoustic velocity

Through analyzing the acoustic velocity and resistivity experiments under different water saturation conditions, the relationship between slowness of P/S wave and resistivity is obtained, as shown in Fig. 2. The resistivity is inversely proportional to the acoustic slowness, which is a power function relationship.

#### (3) Relationship between resistivity and NMR T2 value

In order to research the experimental relationship between the nuclear magnetic resonance  $T_2$  value and  $I$ , which  $I$  is the coefficient of resistance increase in Archie's formula (Archie 1942). The resistivity measurement experiments under the conditions of standard  $T_2$  and different water saturation were used. According to the fractal

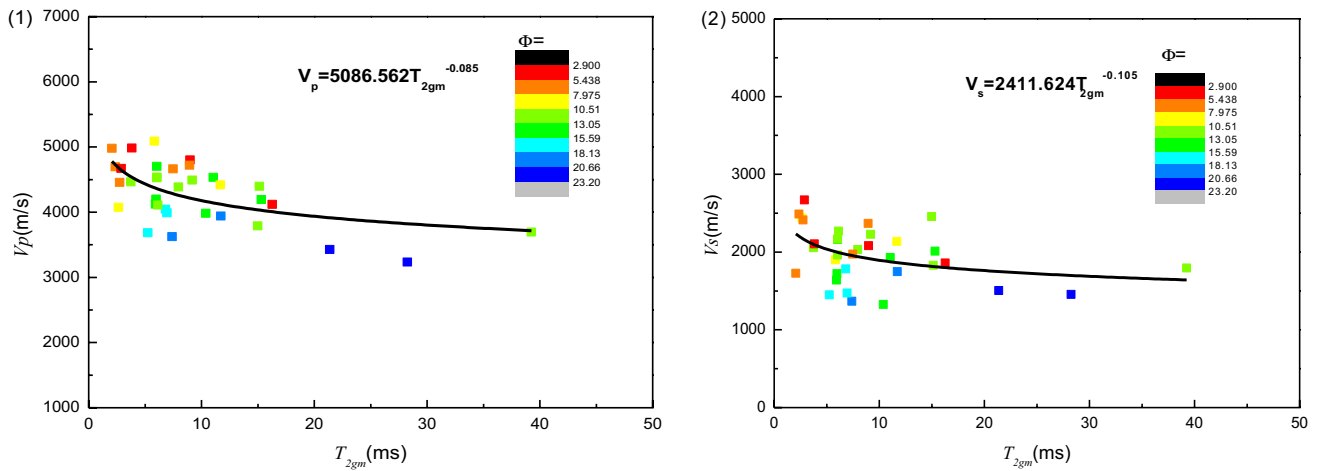


**Fig. 1** (1) The experimental relationship between  $V_p$  and  $T_{2gm}$  (2) The experimental relationship between  $V_s$  and  $T_{2gm}$

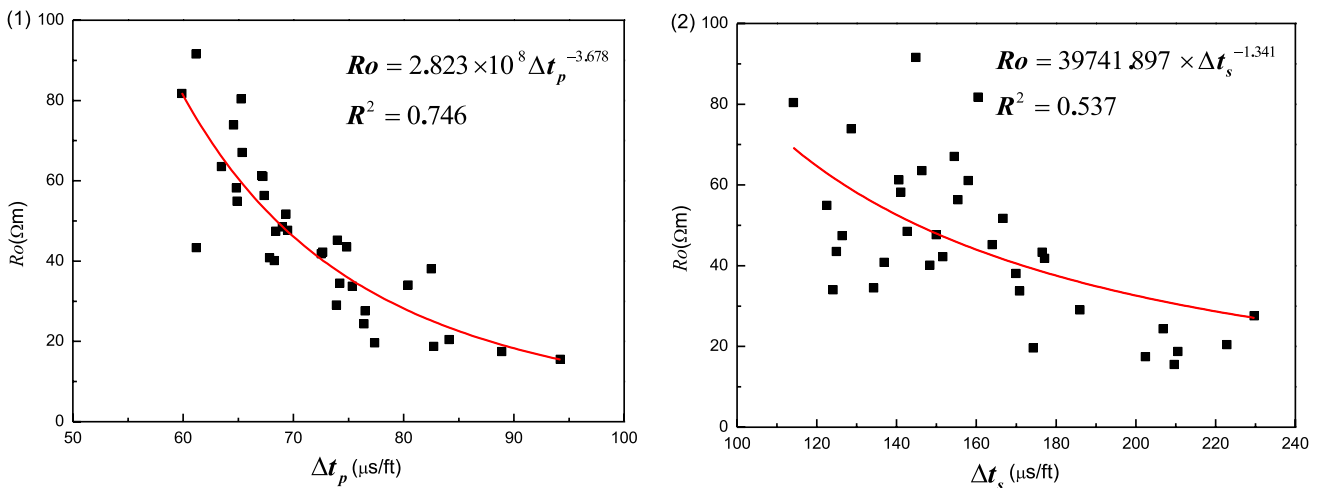


**Fig. 2** (1) The experimental relationship between resistivity and P-wave slowness (2) The experimental relationship between resistivity and S-wave slowness

characteristics of mercury injection curve, the pore structure of samples in the study area is divided into four categories, and the classification results are shown in Fig. 3 and the corresponding NMR spectrum is shown in Fig. 4.

Taking one sample data from each pore structure for research, the NMR T2 spectrum and I-Sw relationship of the four samples are shown in Figs. 5 and 6, respectively. From class I to class IV, the proportion of the large pore component of T2 spectrum decreases, and the slope of the straight line on the I-Sw double logarithm diagram increases.

Fitting  $T_2$  value and  $I$  corresponding to the same water saturation, the result is shown in Fig. 7. It can be seen from the figure that the value of NMR  $T_2$  is inversely proportional to  $I$  and there is a typical power function relationship between them.

## Discussion

### Relation deduction of the relationship between acoustic velocity and NMR T2gm

The relationship between acoustic slowness and porosity is similar to linear relationship, and it is influenced by pore structure. The geometric mean value of NMR  $T_2$  is also a key parameter to characterize pore structure, which is closely related to porosity.

NMR  $T_2$  of rock is affected by pore structure characteristics such as pore morphology (Yan et al. 2017), while the acoustic velocity of rock is affected by pore structure. Previous studies (Deng et al. 2016) have shown that the

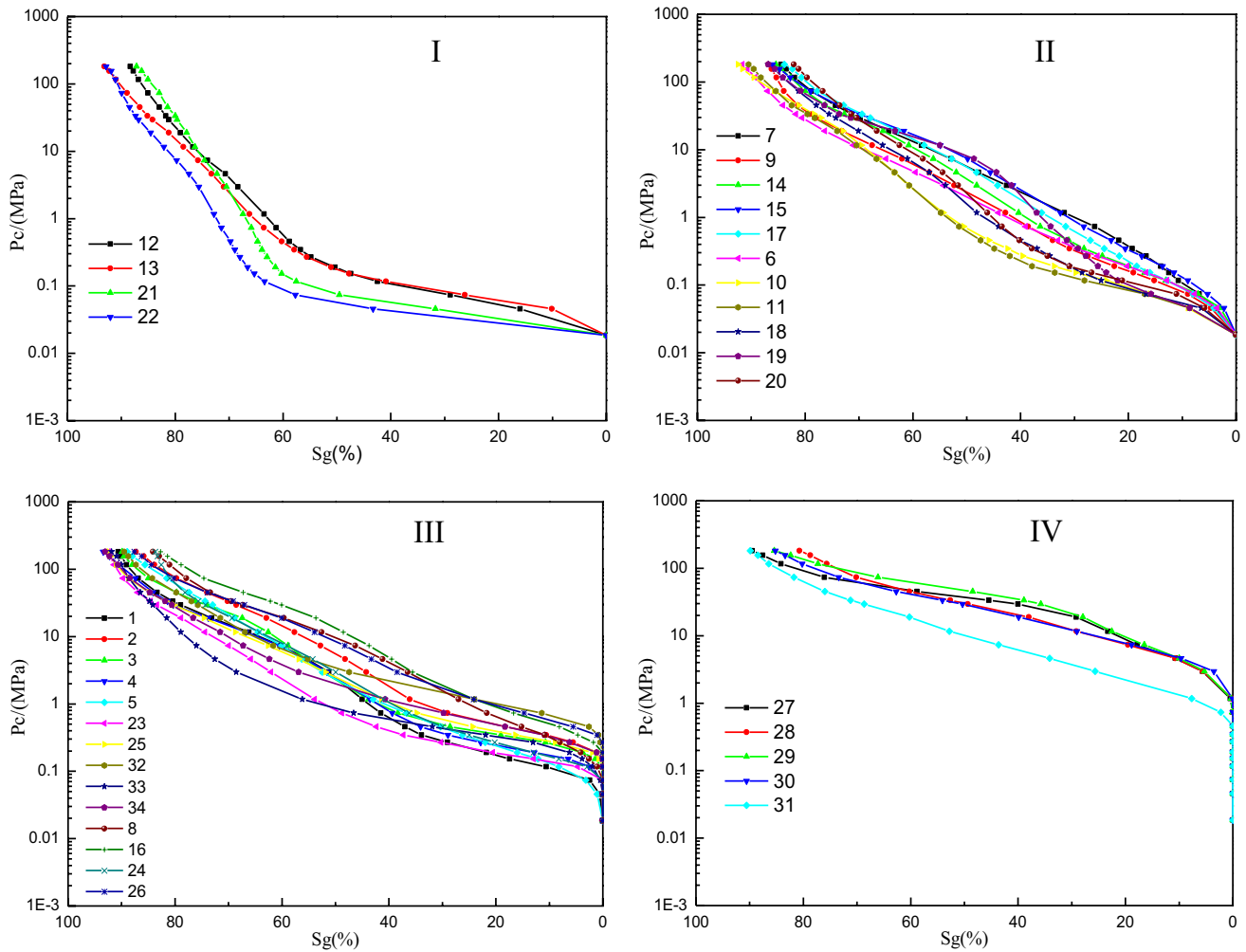


Fig. 3 Classification of pore structure based on mercury intrusion curve morphology

relationship between acoustic velocity and the geometric mean value of NMR  $T_2$  is as follows:

$$v = A \cdot T_{2gm}^{-C} \tag{1}$$

In the formula:  $v$  is acoustic velocity,  $A$  and  $C$  are regional empirical constants which can be obtained by experiments.

In order to study the relationship between acoustic wave velocity and  $T_2$  geometric mean value of NMR, it is assumed that the pores of the rock are all ellipsoids. For ellipsoid pores, the radius of the long axis is  $r$ , the aspect ratio of the pores is  $\alpha$ , and the radius of the two short axes is equal, both of them are  $\alpha r$  (Deng et al. 2016). Then:

$$\frac{1}{T_{2i}} = \rho \left( \frac{S}{V} \right)_i = \rho \frac{4\pi\alpha_i^\beta r_i^2}{4/3\pi\alpha_i^2 r_i^3} = \rho \frac{3\alpha_i^{\beta-2}}{r_i} \tag{2}$$

In the formula:  $T_{2i}$  is the  $T_2$  value of the  $i$ th pore.  $\rho$  is the surface relaxation rate.  $S$  is the pore surface area.  $V$  is the

pore volume.  $r_i$  is the long axis radius of the  $i$ th pore, and  $\beta$  is the coefficient introduced in estimating the pore surface area.

From formula(2), we can get:

$$\frac{r_i}{3\alpha_i^{\beta-2}} = cT_{2i} \tag{3}$$

Take the geometric mean value of the above formula, and then we can get

$$\frac{r}{3\alpha^{\beta-2}} = dT_{2gm} \tag{4}$$

In the formula:  $T_{2gm}$  is the geometric mean value of  $T_2$ ;  $r$  is the equivalent long axis radius;  $\alpha$  is the equivalent pore aspect ratio;  $d$  is the coefficient, which is related to porosity and other factors.

There are some experiments showing that (Yang et al. 2014):

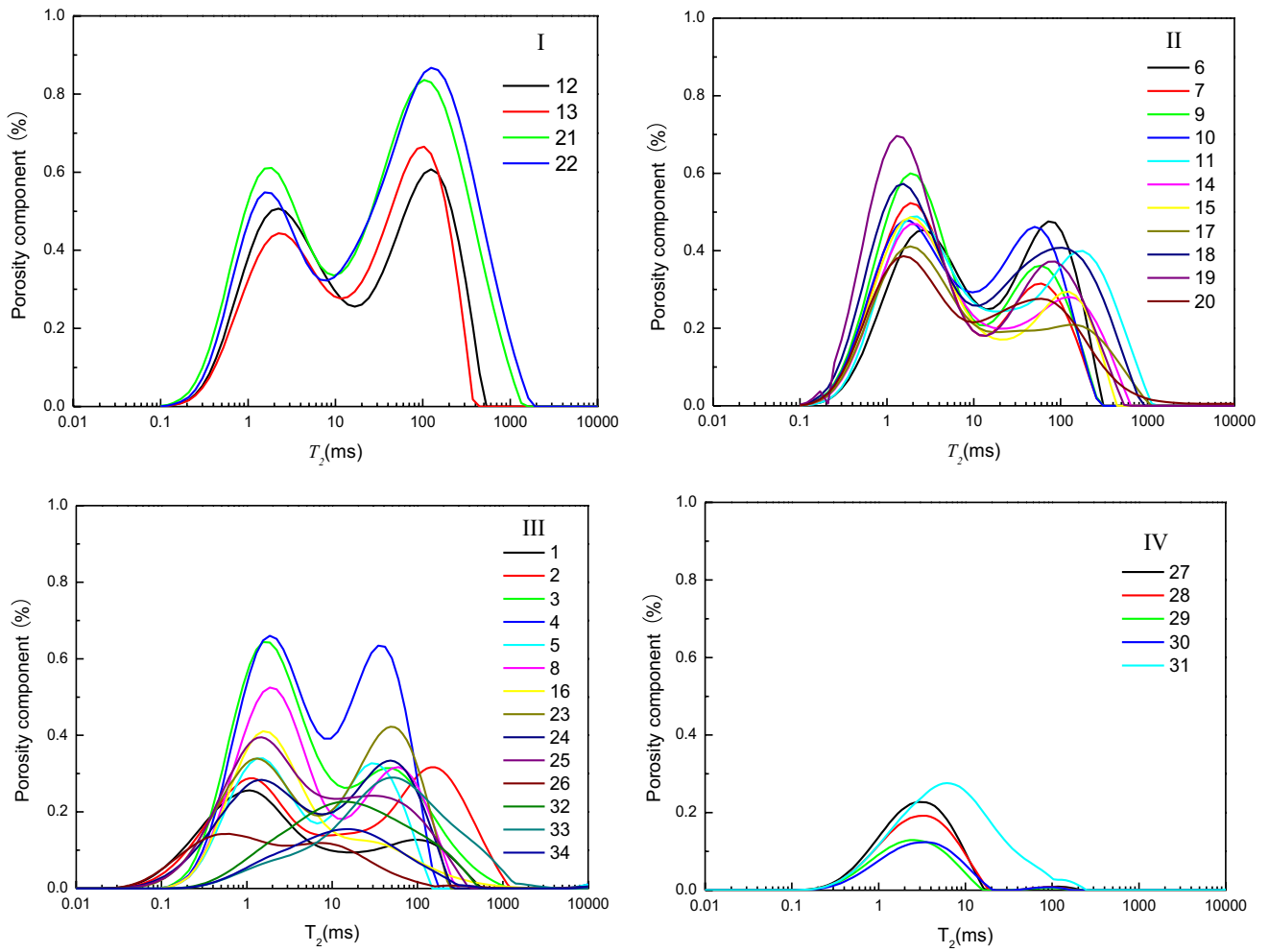


Fig. 4 NMR  $T_2$  spectra of rocks with different pore structures

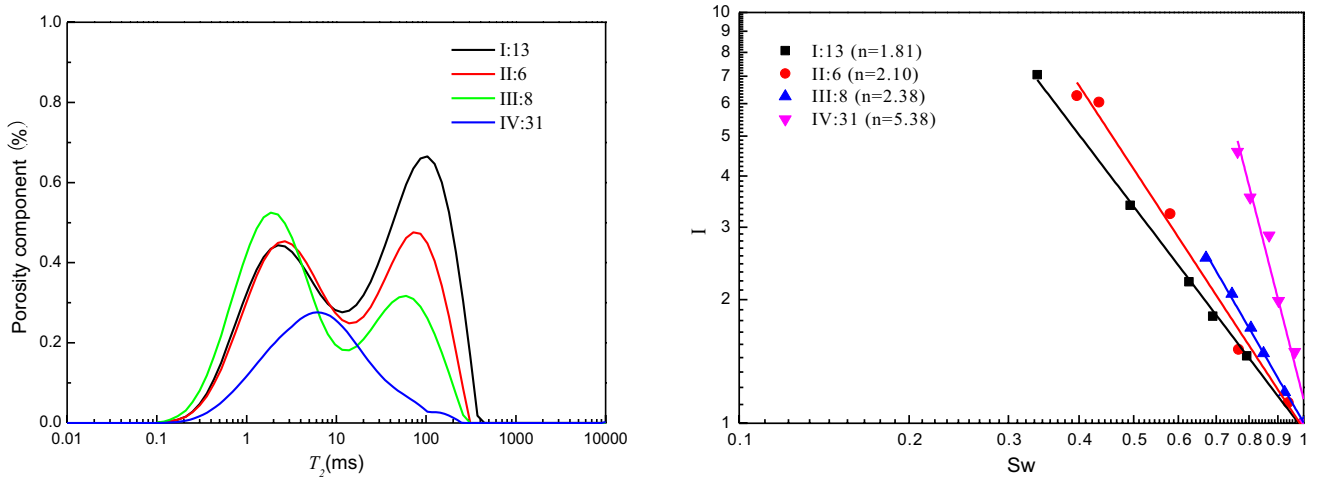


Fig. 5 NMR  $T_2$  spectrum of four samples

Fig. 6  $I-S_w$  of four samples

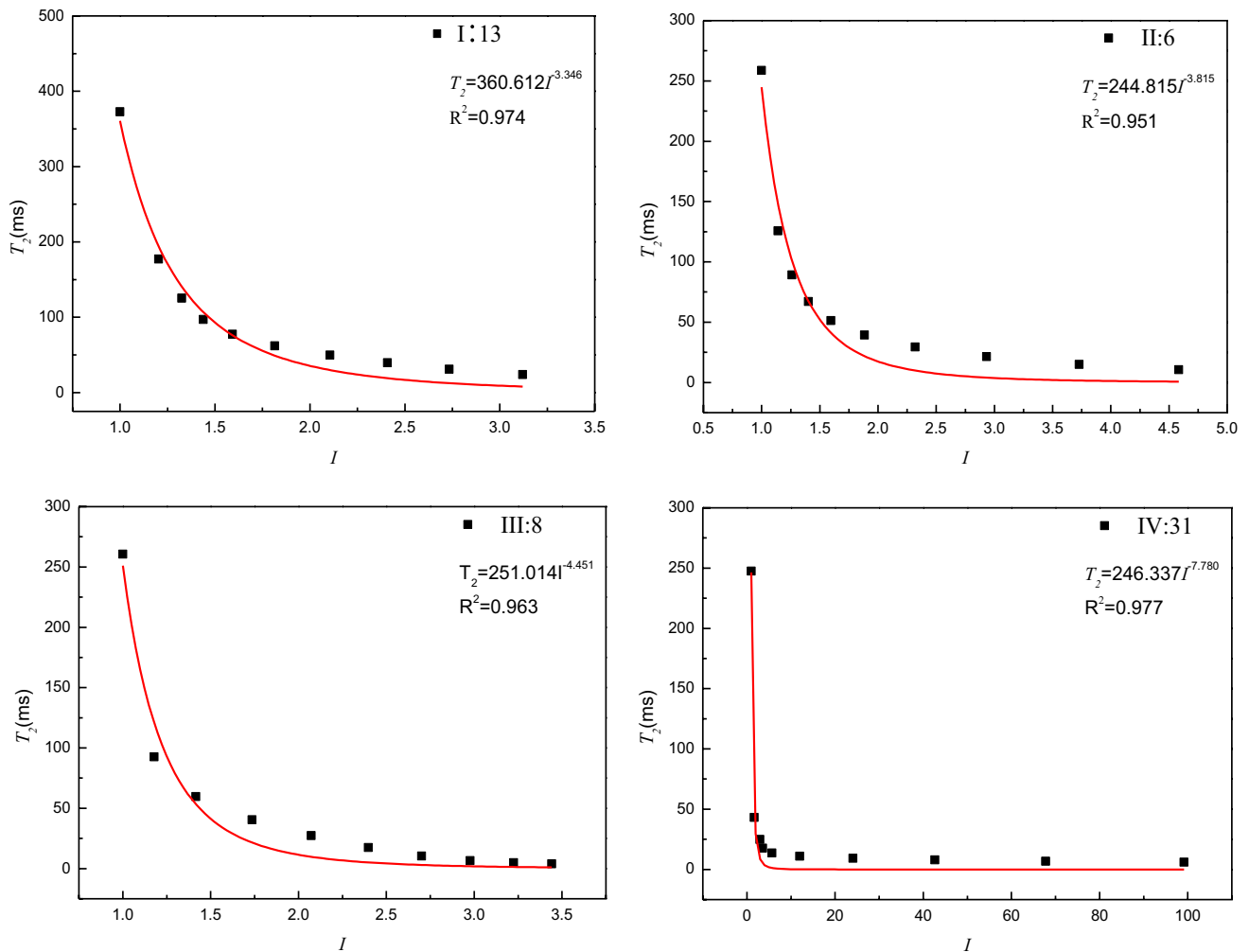


Fig. 7  $T_2$ - $I$  of four samples

$$r_e = \alpha^{\frac{2}{3}} r = c_1 T_{2gm}^{c_2} \tag{5}$$

In the formula:  $r_e$  is the equivalent pore radius;  $c_1$  and  $c_2$  are regional empirical coefficients, which can be obtained by experiments.

By substituting (5) in (4), we can get:

$$\frac{c_1 T_{2gm}^{c_2}}{3\alpha^{\beta-\frac{4}{3}}} = c T_{2gm} \tag{6}$$

From the above formula, we can further get:

$$\alpha = A_1 T_{2gm}^{c_3} \tag{7}$$

In the formula,  $A_1$  and  $c_3$  are regional experience coefficients, which can be obtained by experiments.

The experimental relationship between the geometric mean value of NMR  $T_2$  and the aspect ratio of pores is shown in Fig. 8. There is a direct power function

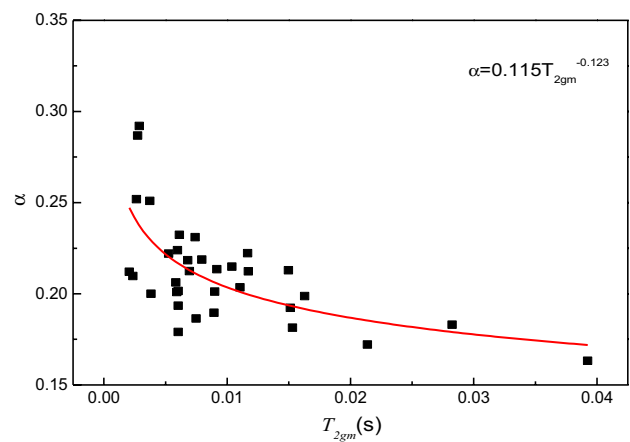


Fig. 8 Relationship between pore aspect ratio and  $T_{2gm}$

relationship between  $\alpha$  and  $T_{2gm}$ , which verifies the above reasoning conclusion. Applying the above relationship

to the differential equivalent medium model (Yang et al. 2014), we can get the relationship between the P/S wave velocity and the geometric mean of the transverse relaxation time of NMR. The parameter is set to  $A_7=0.115$ ,  $c_3=0.123$ , which is determined from Fig. 8. Because the samples in the study area are all sandstone, in the differential equivalent model,  $Km$  are the volume modulus and shear model of rock, respectively, and  $Kf$  is the volume modulus of fluid, the parameters are set as  $Km=37GPa$ ,  $Gm=44GPa$ ,  $Kf=2.19GPa$ ,  $S_w=1$ , which are the theoretical value of sandstone. The relationship between P/S wave velocity and the geometric mean of  $T_2$  is shown in Fig. 9. It can be seen from the figure that under the same porosity, the velocity of P/S wave is inversely proportional to that of  $T_{2gm}$ , which is a power function relationship. Under the same  $T_{2gm}$  conditions, the smaller the porosity is, the larger the P/S wave velocity is. The above simulation results explain the distribution of experimental data in Fig. 1.

### Exploration the empirical relationship between acoustic wave velocity and resistivity

The relationship between acoustic slowness and resistivity has been concerned for a long time (Wei. 1991), and there is a power function empirical relationship between P-wave velocity and resistivity, which is affected by burial depth. The study of the empirical relationship between acoustic wave velocity and resistivity can provide a reference for the comprehensive use of acoustic and resistivity data for fluid identification and shear wave prediction.

In the classical physical volume model of rock, the formula of rock porosity obtained from the response of acoustic slowness without considering argillaceous is:

$$\phi = \frac{\Delta t - \Delta t_{ma}}{(1 - S_w)\Delta t_g + S_w\Delta t_w - \Delta t_{ma}} \tag{8}$$

In the formula:  $S_w$  is water saturation;  $\Delta t$  is the measured acoustic slowness;  $\Delta t_{ma}$  is the acoustic slowness of rock skeleton;  $\Delta t_w$  is the slowness of formation water acoustic wave;  $\Delta t_g$  is the acoustic slowness of natural gas.

According to the relation between porosity and resistivity in Archie formula (Archie 1942), we can get:

$$R_t = \frac{abR_w}{\left(\frac{\Delta t - \Delta t_{ma}}{(1 - S_w)\Delta t_g + S_w\Delta t_w - \Delta t_{ma}}\right)^m} / S_w^n \tag{9}$$

which  $a$  and  $b$  are coefficients of Archie’s formula,  $m$  is cementation index,  $n$  is saturation index, and  $R_w$  is formation water resistivity.

It can be seen from the above formula that the relationship between formation resistivity and P-wave slowness should be power function. This relationship is affected by the water saturation of the stratum.

Shear wave and porosity are related to each other in sandstone, and it is believed that there is an empirical relationship between S-wave slowness and porosity (MedlIn 1993):

$$\phi = c\Delta t_s + d \tag{10}$$

In the formula,  $c$  and  $d$  are coefficients.

According to Archie formula (Archie 1942), the relation between S-wave slowness and resistivity can be obtained from formula (13):

$$R_t = \frac{abR_w}{(c\Delta t_s + d)^m} / S_w^n \tag{11}$$

Based on the above theoretical derivation and internationally accepted sandstone skeleton value, we take

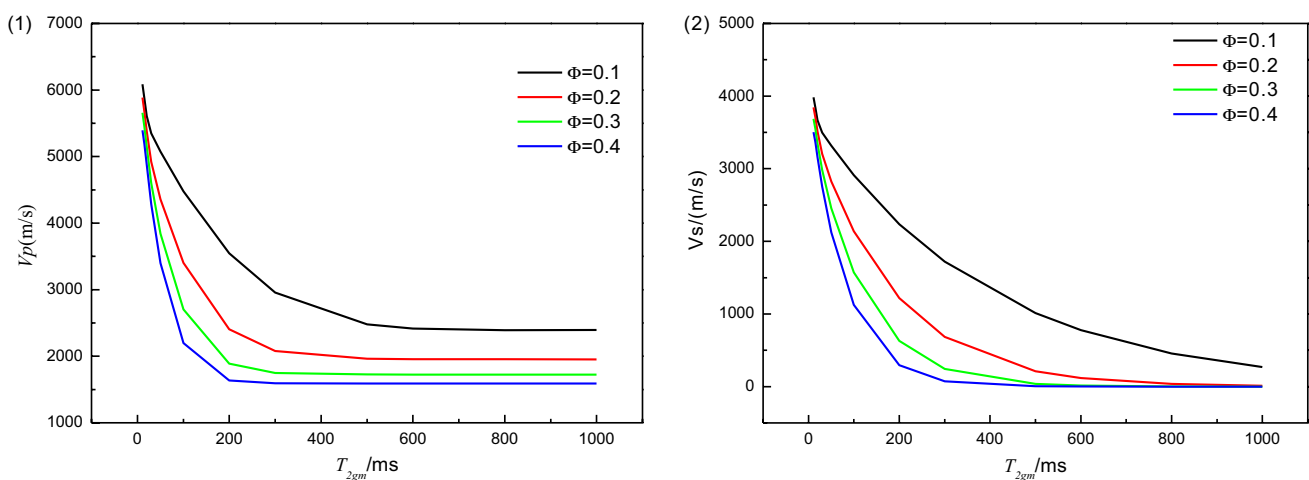


Fig. 9 The theoretical relationship between  $V_p$ ,  $V_s$  and  $T_{2gm}$  (1)  $V_p$  and  $T_{2gm}$ , (2)  $V_s$  and  $T_{2gm}$

$\Delta t_w = 189 \mu\text{s}/\text{ft}$ ,  $\Delta t_{ma} = 56 \mu\text{s}/\text{ft}$ ,  $\Delta t_g = 896 \mu\text{s}/\text{ft}$ ,  $a = b = 1$ ,  $m = 1.8$ ,  $n = 2$ ,  $R_w = 1.326 \Omega\cdot\text{m}$ ,  $c = 0.12$ ,  $d = -7.2$ . According to the simulation of formula (9) and formula (11), different water saturation conditions are obtained. The relationship between resistivity and slowness of P-wave and S-wave is shown in Figs. 10 and 11. It can be seen from the figures that there is a power function relationship between resistivity and slowness of P-wave and S-wave. With the same acoustic slowness, the smaller the water saturation is, the greater the resistivity and the smaller the slowness between water saturation and acoustic wave. Such rocks tend to have the largest apparent resistivity. This is consistent with the conventional understanding, and this result also verifies the reliability of the fitting relation in Fig. 2.

### Derivation of the theoretical relationship between resistivity and NMR T2 value

The conductivity of rock is closely related to its pore structure, and the NMR  $T_2$  spectrum is a direct reflection of the pore structure of rocks (Guo et al. 2019). Therefore, there is an inevitable theoretical relationship between the resistivity of rocks and the distribution of NMR  $T_2$  spectrum. It is convenient for quantitative analysis of saturation index to study the relationship between the two, especially the relationship between  $T_2$  spectrum and resistivity index (Ge et al. 2012).

Mercury injection curve has fractal characteristics, which can be expressed as follows:

$$\lg(S_w) = (3 - D) \lg P_0 + (D - 3) \lg P_c \tag{12}$$

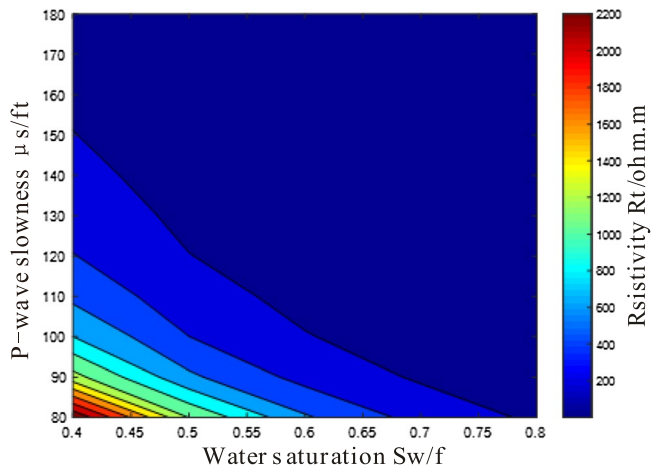
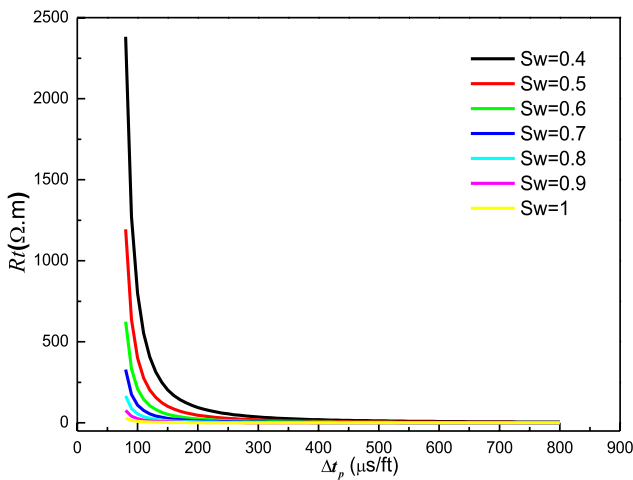


Fig. 10 Relationship between resistivity and P-wave slowness

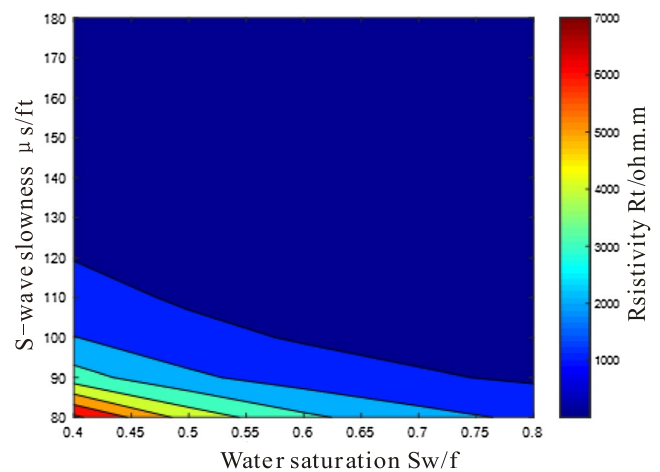
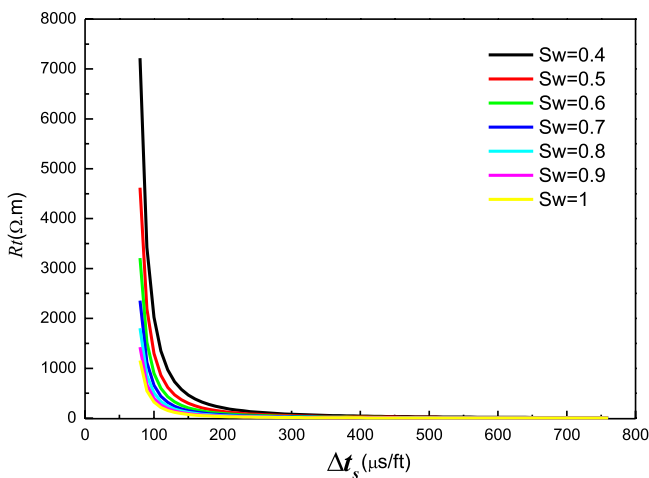


Fig. 11 Relationship between resistivity and S-wave slowness



In the formula:  $D$  is the fractal dimension;  $P_c$  is the pressure;  $P_0$  is the capillary pressure when the rock is 100% water cut;  $S_w$  is the water saturation.

From Archie formula (Archie 1942) and the formula (12), we can get:

$$P_c = P_0 I^\delta \tag{13}$$

In the formula:  $\delta$  is a parameter whose value is related to the water film thickness.

According to previous studies, the relationship between Mercury injection capillary pressure and  $T_2$  value is a power function (He et al. 2005), which can be obtained by combining with the above formula:

$$T_2 = a \frac{1}{I}^{n_I - T_2} \tag{14}$$

In the formula:  $a$  and  $n_I - T_2$  are the fitting coefficients.

It can be concluded from formula (14) that there is a power function relationship between the value of NMR  $T_2$  and the increase rate of rock resistance.

The  $T_2$  cumulative spectrum and  $I-S_w$  data of NMR were processed by three times of spline interpolation, and the NMR  $T_2$  and  $I$  values with corresponding relationship under the same water saturation were obtained. The relationship between the NMR  $T_2$  and water saturation of the above 4 samples is shown in Fig. 12. It can be seen from the figure that  $T_2$  and  $I$  have a good correlation with water saturation after interpolation.  $I$  decreases with the increase in water saturation, but  $T_2$  increases with the increase in water saturation. In addition, there is a power function relationship among  $T_2$ ,  $I$  and water saturation, which shows that there is a certain relationship between  $T_2$  and  $I$ . It can be seen from the figure that  $T_2$  and  $I$  have a good correlation with water saturation after interpolation.  $I$  decreases with the increase in water saturation, and  $T_2$  increases with the increase in water saturation. Moreover, it appears that there is an obvious power function relationship among  $T_2$ ,  $I$  and water saturation, which indicates that there is a certain relationship between  $T_2$  and  $I$ .

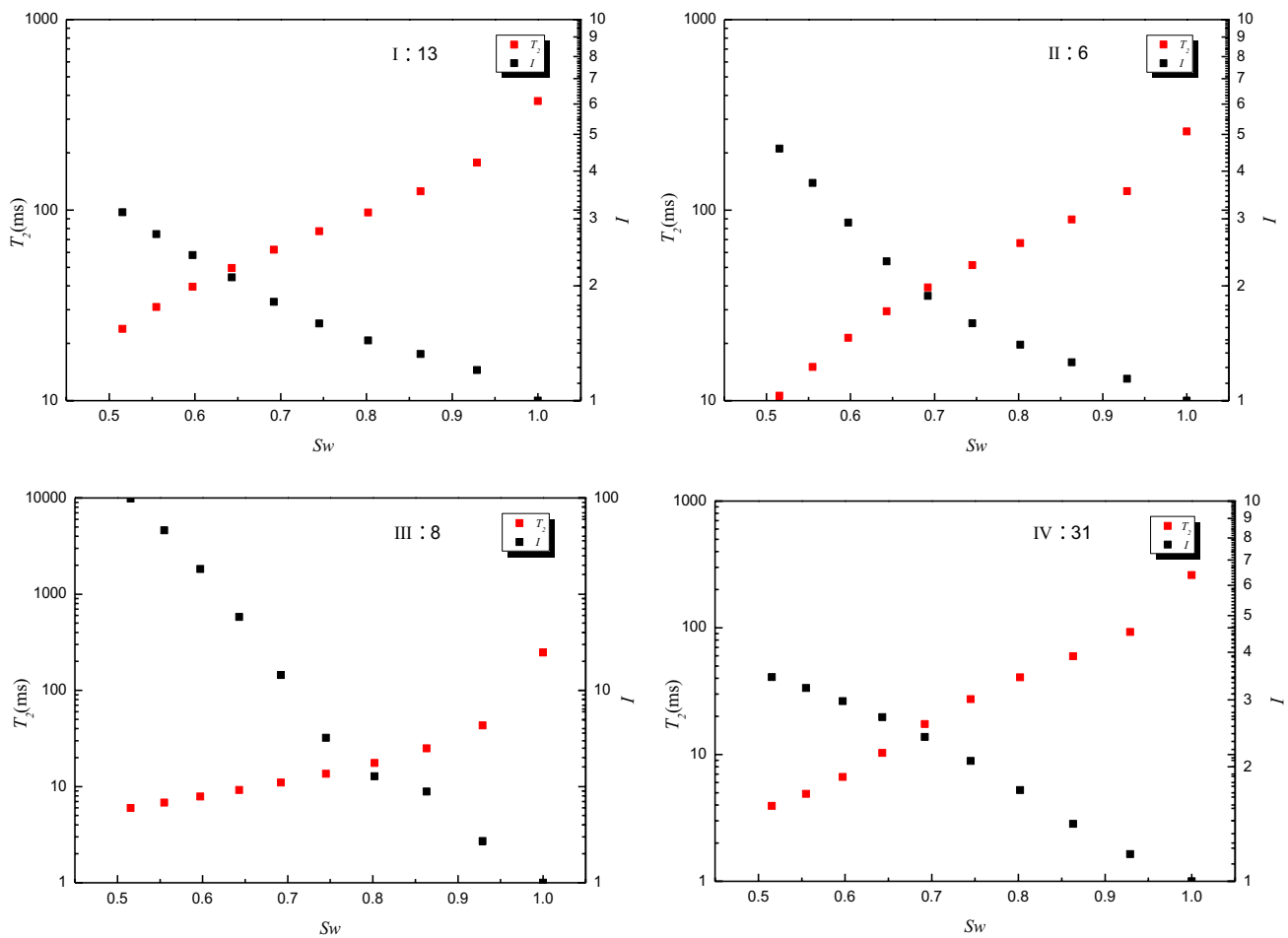


Fig. 12  $T_2$ - $I$ - $S_w$  of four samples

## Multi-parameter joint-identification of gas bearing reservoir

At present, the gas bearing identification of reservoir is mainly based on the intersection of conventional logging information, and there are still deficiencies in the application of new logging technology and multi-information joint-application (Bian et al. 2014; Guo et al. 2018). According to the previous study, the relationship among acoustic, resistivity and NMR properties is established through the pore structure. The combination of acoustic, resistivity and nuclear magnetic information has a good effect on gas bearing identification. Figure 13 is the chart of gas bearing property identified by the intersection of P/S velocity ratio and acoustic slowness of well G in the study area and the chart of gas bearing property identified by the joint intersection of acoustic resistivity nuclear magnetic. Figure 14 is the logging curve of reservoir section of well G. It can be seen from the comparison that the separation effect of gas and water in the gas bearing identification plate based on the acoustic resistivity nuclear magnetic resonance is more obvious than that based on the velocity ratio of P/S wave and the slowness of P/S wave. The gas test results of three reservoirs show that the gas production per day before fracturing is 130000 m<sup>3</sup>. In this paper, the gas bearing property is not considered in the transformation of acoustic wave. However, in fact, if the gas bearing resistivity is too large, the transformation term ( $T_{2gm}^{0.105}/R_{tx}^{-0.272}$ ) which is obtained from Figs. 1b and 2a will be reduced, while the water layer data will not change much. This enlarges the difference between gas and water data points, so the established plate has better recognition effect on gas bearing property of tight reservoir. In the conversion term, because of the relationship between the shear wave velocity obtained in the first section and  $T2gm$  (geometric mean of  $T2$ ),  $T2gm$  is used instead of the shear wave

velocity in the molecular part. In the denominator part, the relation between the P-wave and the resistivity obtained in the second section of the paper is used to replace the S-wave with the resistivity. Among them,  $R_{tx} = Rt/2.823 \bullet 108$ ,  $Rt$  is the measured resistivity of the formation.

## Conclusion

- (1) The pore aspect ratio is a power function of  $T_{2gm}$ . Under the same porosity, the velocity of P/S wave is inversely proportional to  $T_{2gm}$ , which is a power function relationship. Under the same  $T_{2gm}$ , the smaller the porosity is, the larger the P/S wave velocity is. Under the condition of the same water saturation, the relation between resistivity and slowness of P/S wave is power function, which can provide reference for the prediction of S-wave.
- (2) There is an obvious power function relationship among  $T_2$ ,  $I$  and water saturation. The  $T_2$  value of NMR is inversely proportional to  $I$ , and the relationship between them is a typical power function. In the fitting relationship between the NMR  $T_2$  value and the resistivity increasing coefficient  $I$ , the coefficient  $n_I T_2$  has a linear relationship with the saturation index  $n$  and a power function relationship with the water film thickness. This relationship is of great significance to the construction of new interpretation models of saturation and permeability.
- (3) The result of gas bearing identification by combining acoustic, resistivity and nuclear magnetic information is better than that by conventional gas bearing identification method, which has certain guiding significance for gas water identification in complex formation.

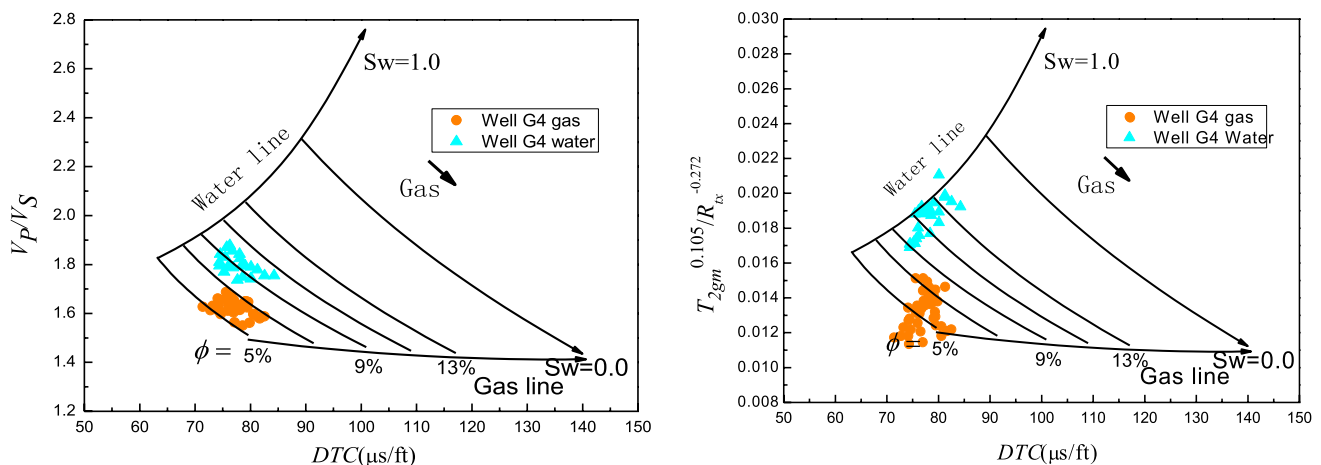


**Fig. 13** (1) Gas identification cross-plot of G4 well with  $V_p/V_s$  and  $V_p$  (2) Gas identification of G4 well with joint acoustic, resistivity and NMR

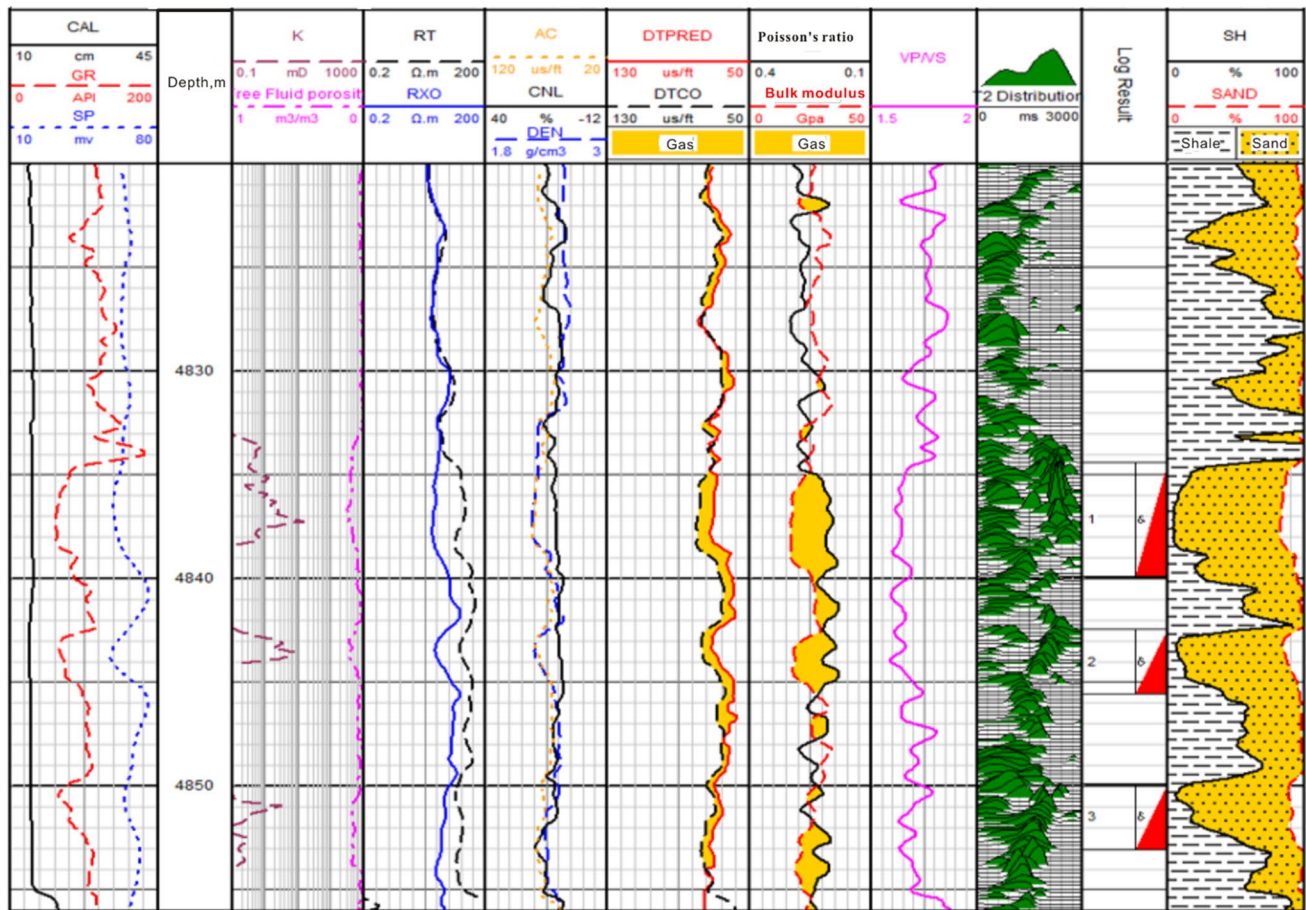


Fig. 14 Logging interpretation results of G well

## Compliance with ethical standards

**Conflict of interest** No conflict of interest exists in the submission of this manuscript, and manuscript is approved by all authors for publication. I would like to declare on behalf of my co-authors that the work described was original research that has not been published previously, and not under consideration for publication elsewhere, in whole or in part. All the authors listed have approved the manuscript that is enclosed.

## References

- Archie GE (1942) The electrical resistivity log as an aid in determining some reservoir characteristics. *Trans Am Inst Mech Eng* 146(01):54–61
- Cao T, Song Z, Wang S, Xia J (2016) Characterization of pore structure and fractal dimension of Paleozoic shales from the northeastern Sichuan Basin, China. *J Nat Gas Sci Eng* 35:882–895
- Changjiang W (1991) Exchange of acoustic wave and resistivity and its application. *Geophys Prospecting Pet* 30(02):115–121
- Chengzu H (1998) The thickness of water in oil and gas reservoir. *Pet Exploration Dev* 25(2):75–77
- Chen HQ, Cao C, Liang SX, Li JH (2013) Research advances on reservoir pores. *Nat Gas Geosci* 24(2):227–237
- Fengming Z, Yue Z, Dongzhi Z, Weibiao X, Mingming M (2016) Prediction method for shear wave velocity based on nmr  $t_2$  geometric average. *Well Logging Technol* 40(1):23–27
- Fengying Y, Xingyao Y, Bo L (2014) The research of variable dry rock matrix equivalent model. *Geophysical Prospecting For Petroleum* 53(3):280–286
- Guo S, Lyu X, Zhang Y (2018) Relationship between tight sandstone reservoir formation and hydrocarbon charging: A case study of a Jurassic reservoir in the eastern Kuqa Depression, Tarim Basin, NW China. *J Nat Gas Sci Eng* 52:304–316
- Guo X, Huang Z, Zhao L, Han W, Ding C, Sun X, Wang R (2019) Pore structure and multi-fractal analysis of tight sandstone using MIP, NMR and NMRC methods: A case study from the Kuqa depression, China. *J Pet Sci Eng* 178:544–558
- Hamada GM, Al-Blehed MS, Al-Awad MN, Al-Saddique MA (2001) Petrophysical evaluation of low-resistivity sandstone reservoirs with nuclear magnetic resonance log. *J Pet Sci Eng* 29(2):129–138
- Han S, Zhang J, Yang C, Bai S, Huang L, Dang W, Wang C (2016) Well log evaluation of shale gas reservoirs and preservation conditions of Lower Cambrian shale succession in Cengong Block of south-east Sichuan basin, south China. *J Nat Gas Sci Eng* 33:337–346
- He YD, Mao ZQ, Xiao LZ (2005) A new method to obtain capillary pressure curve using nmr  $t_2$  distribution. *J Jiling Univ (Earth ence Edition)* 35(2):177–181
- Jianping Y, Xu H, Bin G, Qinhong H et al (2017) Nuclear magnetic resonance T2 spectrum: multifractal characteristics and pore structure evaluation. *Appl Geophys* 14(2):205–215

- Kumar, M., & Han, D. H (2005). Pore shape effect on elastic properties of carbonate rocks. In SEG Technical Program Expanded Abstracts, 1477–1480.
- Liu Y, Tang T, Huanhong Du et al (2013) Study of rock conductive mechanism based on pore structure. *Chinese J Geophys* 56(8):2819–2826
- Li Z, Shen X, Qi Z, Hu R (2018) Study on the pore structure and fractal characteristics of marine and continental shale based on mercury porosimetry, N<sub>2</sub> adsorption and NMR methods. *J Nat Gas Sci Eng* 53:12–21
- MedlIn WL (1993) Shear wave velocity logging in sandstone. *Foreign oil and gas exploration* 5(4):458–466
- Ning, Z. H. , Zhi, T. T. , Yan, L. T. , Pei, S. , & Ming, J. L (2015) A saturation evaluating method based on pore structure. *Progress in Geophysics*.
- Oluwadebi AG, Taylor KG, Ma L (2019) A case study on 3D characterisation of pore structure in a tight sandstone gas reservoir: The Collyhurst Sandstone, East Irish Sea Basin, northern England. *Journal of Natural Gas Science and Engineering* 68:102917
- Prasad M (2001) Mapping impedance microstructures in rock with acoustic microscopy. *Lead Edge* 20(2):172–179
- Shaogui D, Yunfeng N, Yue Z et al (2016) Nuclear magnetic resonance-acoustic velocity joint experiment of tight gas sandstone. *Acta Petrolei Sinica* 37(06):768–776
- Tangyan L, Yan J, Yan J, Feng X, Zaitian M (2012) Theoretical mechanism and application of sphere–cylinder model in nmr for oil–water porous media. *Pure Appl Geophys* 169(7):1257–1267
- Verwer K, Eberli GP, Weger RJ (2011) Effect of pore structure on electrical resistivity in carbonates. *AAPG Bull* 95(2):175–190
- Wang Z, Xiao L, Liu T (2004) A new method for multi-exponential inversion of nmr relaxation measurements. *Sci China, Ser G* 47(3):265–276
- Wei C (1991) Exchange of acoustic wave and resistivity and its application. *Geophys Prospecting Pet* 30(02):115–121
- Wyllie MRJ, Gregory AR, Gardner LW (1956) Elastic wave velocities in heterogeneous and porous media. *Geophysics* 21(1):41–70
- Xinmin G, Yiren F, Fei W et al (2012) Correspondence of core nuclear magnetic resonance T<sub>2</sub> spectrum and resistivity index. *J China Univ Pet*, 36(06):53–56+51.
- Xu Y, Wang Y, Yuan H, Zhang D, Agostini F, Skoczylas F (2018) Pore structure characterization of tight sandstone from Sbaa Basin, Algeria: investigations using multiple fluid invasion methods. *J Nat Gas Sci Eng* 59:414–426
- Yang F, Yin X, Liu Bo (2014) The research of variable dry rock matrix equivalent model. *Geophys Prospecting Pet* 53(3):280–286
- Yan W, Sun J, Cui L, Yan G (2017) A new method of estimating nmr t<sub>2</sub> spectrum of sandstone. *Journal of China University of Petroleum (Edition of Natural Science)* 41(1):60–68
- Yin S, Ding W, Zhou W, Shan Y, Wang R, Liu J, Gu Y (2016) Logging assessment of tight clastic rock reservoir fractures via the extraction of effective pore aspect ratios: A case study of lower Permian strata in the southern Qinshui Basin of eastern China. *Journal of Natural Gas Sci Eng* 36:597–616
- Yuanhui B, Fei W, Chongwang Y et al (2014) Fluid property of tight sandstone reservoir identified with elastic parameters. *J Earth Sci Environ* 36(4):99–106
- Yudan H, Zhiqiang M, Lizhi X et al (2005) A new method to obtain capillary pressure curve using NMR T<sub>2</sub> distribution. *Journal of Jilin University (Earth science edition)* 35(2):177–181
- Yuhang G, Baozhi P, Lihua Z, Chuanhui F (2018) Research and application of the relationship between transverse relaxation time and resistivity index in tight sandstone reservoir. *J Pet Sci Eng* 160:597–604
- Zhang L, Pan B, Shan G, Liu S, Guo Y, Fang C (2017) Probability distribution method based on the triple porosity model to identify the fluid properties of the volcanic reservoir in the Wangfu fault depression by well log. *Comput Geosci* 21(2):241–246
- Zhu P, Lin C, Ren H, Zhao Z, Zhang H (2015) Micro-fracture characteristics of tight sandstone reservoirs and its evaluation by capillary pressure curves: a case study of Permian sandstones in Ordos Basin, China. *J Nat Gas Sci Eng* 27:90–97